Identification of A Transient Neutron Star in Quiescence in the Globular Cluster NGC 5139

Robert E. Rutledge[1], Lars Bildsten[2], Edward F. Brown[3], George G. Pavlov[4], and Vyacheslav E. Zavlin[5]

Received _____; accepted _____

[1] Space Radiation Laboratory, California Institute of Technology, MS 220-47, Pasadena, CA 91125; rutledge@srl.caltech.edu

[2] Institute for Theoretical Physics and Department of Physics, Kohn Hall, University of California, Santa Barbara, CA 93106; bildsten@itp.ucsb.edu

[3] Enrico Fermi Institute, University of Chicago, 5640 South Ellis Ave, Chicago, IL 60637; brown@flash.uchicago.edu

[4] The Pennsylvania State University, 525 Davey Lab, University Park, PA 16802; pavlov@astro.psu.edu

[5] Max-Planck-Institut für Extraterrestrische Physik, D-85740 Garching, Germany; zavlin@xray.mpe.mpg.de

ABSTRACT

Using the *Chandra*/ACIS-I detector, we have identified an X-ray source (CXOU 132619.7-472910.8) in the globular cluster NGC 5139 with a thermal spectrum identical to that observed from transiently accreting neutron stars in quiescence. The absence of intensity variability on timescales as short as 4 seconds ($< 25\%$ rms variability) and as long as 5 years ($<50\%$ variability) supports the identification of this source as a neutron star, most likely maintained at a high effective temperature ($\approx 10^6$ K) by transient accretion from a binary companion. The ability to spectrally identify quiescent neutron stars in globular clusters (where the distance and interstellar column densities are known) opens up new opportunities for precision neutron star radius measurements.

1. Introduction

The large number of low luminosity X-ray sources (LLXS; $L_X \lesssim 10^{34}$ erg s^{-1}) in globular clusters (GCs) were initially explained as accreting white dwarfs (Hertz & Grindlay 1983), although some fraction may be active RS CVn binaries (Bailyn et al. 1990). Some of these systems may also be transient neutron stars in quiescence (qNSs; Verbunt et al. 1984). The observations of transient neutron stars in outburst in globular cluster NGC 6440 (Forman et al. 1976; in 't Zand et al. 1999; Verbunt et al. 2000) and in Liller 1 (Lewin et al. 1976), supports the suggestion that such a population exists in globular clusters. We report here on our spectral search for such an object within the globular cluster NGC 5139(ω Cen).

Much observational and theoretical work has been carried out on accreting transients in the field, most of which are black holes. The quiescent emission from neutron stars has been well observed, resulting in numerous models for the source of the quiescent emission, ranging from accretion in quiescence to thermal emission from the NS surface (see Bildsten & Rutledge 2000 for an overview). Brown, Bildsten & Rutledge (1998, BBR98 hereafter) showed that the neutron star (NS) core is heated by reactions deep in the NS crust during the repeated accretion outbursts common in transients (for reviews of transient neutron stars, see Chen et al. 1997; Campana et al. 1998a). The core is heated to a steady-state temperature on a timescale of $\sim 10^4$ yr (see also Colpi et al. 2000), providing an emergent thermal luminosity (BBR98):

$$L_q = 8.7 \times 10^{33} \left(\frac{\langle \dot{M} \rangle}{10^{-10} M_\odot \mathrm{yr}^{-1}} \right) \frac{Q}{1.45 \mathrm{MeV}/m_p} \ \mathrm{ergs\ s}^{-1} \tag{1}$$

where Q is the nuclear energy release in the crust (Haensel & Zdunik 1990).

The soft X-ray spectral component of quiescent neutron stars is expected to be an emergent H atmosphere spectrum (BBR98; for calculations of these spectra, see Rajagopal & Romani 1996; Zavlin et al. 1996). Spectral fits assuming a H atmosphere spectrum yield

emission areas consistent with a NS (Rutledge et al. 1999, 2000, 2001a, 2001b). In addition, a hard spectral component often dominates the spectrum above 2 keV in the two field qNSs Cen X−4 (Asai et al. 1996b; Asai et al. 1998; Campana et al. 2000; Rutledge et al. 2001b) and Aql X−1 (Campana et al. 1998b; Rutledge et al. 2001a), the origin of which is still not clear (Campana et al. 1998a).

We have examined archived *Chandra*/ACIS-I observations of the globular cluster NGC 5139 to spectrally identify qNSs. One X-ray source stands out as having a spectrum consistent with that from a pure hydrogen atmosphere of a 10 km neutron star. This source is also spectrally inconsistent with millisecond radio pulsars (MSPs), cataclysmic variables (CV), or RS CVn binaries. An interpretation of this source as a narrow line Seyfert 1 (NLSy1) is not favored, as it requires an atypical X-ray spectrum for this class, and requires accepting as a coincidence that the intensity should be the same as from a 10 km neutron star at the distance of NGC 5139.

In § 2 we describe the observation and spectral analysis of the point sources in the field of NGC 5139, comparing the X-ray spectra to models appropriate to MSPs, CVs, RS CVns and NLSy1s. We examine previous observations of the identified qNS in § 3, and conclude in § 4 with a discussion.

2. Observation and Point Sources

The *Chandra*/ACIS-I detectors observed NGC 5139 in imaging mode for two continuous periods (2000 Jan 24 02:15-09:46 and Jan 25 04:33-17:24 TT) for a total exposure of ≈ 68.6 ksec. We combined the two observations and analyzed them as one, using CIAO v2.1[6] and XSPEC v11 (Arnaud 1996). We searched for point sources using *celldetect*, using only

[6]http://asc.harvard.edu/ciao/

the 0.1-2.5 keV energy range, excluding regions <16 pixels from the detector edges, and keeping only sources with S/N>5.0. We find 40 X-ray point sources over the four ACIS-I chips and chip S2 of ACIS-S, which are numbered in order of decreasing S/N in Table 1. X-ray point-source counts from extra-galactic deep surveys (Hasinger et al. 1998; Giacconi et al. 2001) imply about 40 background sources total in the 345 sq arcmin region, down to the approximate limit of our sample, 2.6×10^{-15} erg cm^{-2} s^{-1}(0.5-2 keV). Hence, only a fraction of the detected sources are likely to be members of the GC.

We excluded the sources #12, 18, 28 and 30 from spectral analysis due to their close proximity (<33 pixels) to the detector edge. We also excluded sources #1, 9, 16, and 36, as these were >12′ off-axis, with large point spread functions offset in position from *celldetect* position by up to 10″perhaps due in part to the low S/N. For all other point sources, we extracted source counts within a radius $r = 2.1 + 0.073(R/1\ \mathrm{arcmin})^{2.32}$ arcsec where R is the distance from the ACIS-I aimpoint; this is slightly larger than the 90% enclosed energy radius at 6 keV. Background counts were extracted from an annulus centered on the source position, with an inner radius 2 pixels larger than the source region, and an outer radius which was the larger of a factor of 3 times the inner-radius, or 50 pixels, excluding overlapping source regions and off-chip regions. We used the script *psextract* to extract the source counts and background, to generate pulse-invariant (PI) spectra for analysis. We binned the PI spectra into four energy bins: 0.5-1 keV, 1-2 keV, 2-5 keV, and 5-10 keV.

Even though most of these sources are bound to be active galaxies, we begin by comparing these X-ray spectra with spectral models for qNSs, CVs, MSPs and RS CVn's. All spectral models include galactic absorption at the optically implied value of $N_{\mathrm{H},22}$=0.09 (Djorgovski & Meylan 1993), which is comparable to the 21 cm line value (Dickey & Lockman 1990). We assume a fiducial distance to NGC 5139 of 5 kpc, between the extremes of 4.9 and 5.3 kpc which are typically quoted (Djorgovski & Meylan 1993; Harris 1996).

We begin by assuming a H atmosphere spectrum and holding R_∞=13 km (R_∞=$R/\sqrt{1-2M/(Rc^2)}$, where R is the proper radius, M is the NS mass, and c is the speed of light). We then spectrally fit the PI spectra of all X-ray sources. Of the 32 spectrally analyzed sources, two (which we label source #3=CXOU 132619.7-472910.8 and #31) were acceptably fit (prob(χ^2_ν)>0.01; $\chi^2_\nu$is the reduced chi-square statistic; Press et al. 1995) with this spectrum. Of the other 30 sources, only two had values of prob(χ^2_ν)>10^{-6}, while the remainder were far below this value and are thus strongly rejected. We include the χ^2_ν values, and the best-fit $kT^\infty_{\rm eff}$ values for sources #3 and 31, in Table 1.

We then permit the value of R_∞ to vary; the results for these fits are shown in Fig. 2. The majority (29 of 32) of X-ray sources are spectrally hard, and have best-fit $R_\infty \ll 1$ km. Only source #3 overlaps with the ($kT^\infty_{\rm eff}$,R_∞) parameter space of field qNSs. Two other spectrally soft objects (#21 and #31) are observed, but do not produce R_∞ consistent with that of a neutron star. We show a pulse-height amplitude (PHA) spectrum for source #3 in Fig. 1.

As shown previously (see references below), *Chandra* CCD spectroscopy has confirmed that millisecond radio pulsars are detectable in X-rays as power-law sources (Pooley et al. 2000; Grindlay et al. 2001). We also modelled sources #3 and 31 with an absorbed power-law. Source #3 did not produce an acceptable fit (χ^2_ν=12.8/2 dof; prob=3×10^{-6}). Source #31 obtained an acceptable fit, but with a photon power-law slope steeper than observed from MSPs (3.05±0.35 vs. ≈1–2; Saito et al. 1997; Zavlin & Pavlov 1998; Rots et al. 1998; Takahashi et al. 1998; Mineo et al. 2000). (Alternatively, at least one MSP can be described as a thermal polar cap with a H atmosphere spectrum, with a polar cap radius of $\sim$ 1 km [Zavlin & Pavlov 1998], considerably smaller than the H atmosphere radii found from field sources). We exclude an MSP origin for both objects.

To compare the spectra with those of CVs, we obtained best-fit optically thin thermal bremsstrahlung (OTTB) spectral fits for sources #3 and 31 with $N_{\rm H}$ fixed at its optically implied value, extracting the model parameters $kT_{\rm bremss.}$ and $EM(=\int n_e n_p dV)$ for comparison with values of other CVs from Eracleous et al. (1991; E91 hereafter). Results are shown in Fig. 3. Source #3 is spectrally softer than all CVs observed by E91, while having the second highest EM. Source #31 is consistent with being inside the CV parameter space. We exclude a CV origin for source #3, and note the spectral consistency of source #31 with a CV.

For sources #3 and #31, we also fit 2 temperature Raymond-Smith (2T RS) spectral models, as typically observed from RS CVns (Swank et al. 1981; Lemen et al. 1989; Dempsey et al. 1993), holding $Z = 0.019 Z_{\odot}$, which is the mode of metalicities from cluster stars (Majewski & et. al. 1999; Lee et al. 1999). We compare our 2T RS spectral parameters (kT_1, EM_1, EM_2/EM_1) with the spectral parameters for ∼40 field RS CVns measured by Dempsey et al. (1993), D93 hereafter. We hold the high temperature kT_2 fixed at the average value found by D93 (1.4 keV), and permit the remaining parameters to vary. We find no acceptable parameter space within ($0.1< kT_1 < 1.0$ keV, $EM_1 <\times 10^{54}$ cm^{-3}, and $EM_2/EM_1 >1$) in source #3 (best fit values: $kT_1 = 0.42 \pm 0.03$ keV, EM_1=1170^{+190}_{-160} 10^{53} cm^{-3}; $EM_2/EM_1 < 0.016$ 90% confidence upper-limit). In Fig. 4, we show the best-fit spectral parameters of sources #3 and #31 with those of D93. These are clearly distinct from the spectral parameters of RS CVns, while in source #31, they are perhaps comparable.

The NLSy1s are unusual as AGNs, as they have soft X-ray energy spectra (Boller et al. 1996) . The prevalence of NLSy1s in X-ray fields has been estimated at the ∼few per cent level (Hasinger et al. 2000), which is consistent with 1-2 such objects in the NGC 5139 field. NLSy1s are typically (although not always) acceptably modelled with a

single photon power-law of slope α=3-4, with no absorption above that due to the Milky Way, even of high S/N X-ray spectra observed with *ROSAT*/PSPC, such as I Zw 1 and Mrk 1044A (Boller et al. 1996). Source #3, however, is not acceptably fit with a pure power-law spectrum at the galactic absorption (see above), and therefore it would have an unusual X-ray spectrum for a NLSy1. In addition, accepting the hypothesis that source #3 is a NLSy1 requires accepting as a coincidence that the spectral intensity corresponds to an R_∞=13 km object for a H atmosphere spectrum. Both the spectrum and intensity are explained naturally under the qNS hypothesis, and we therefore favor the interpretation of source #3 as a qNS. A definitive exclusion of a NLSy1 origin will require HST imaging and spectroscopy of objects in the X-ray error box. Presently available HST observations of NGC 5139 do not include source #3.

The 3σ upper-limit on the 0.5-10 keV luminosity of an $\alpha = 1$ power-law component is <12% of the thermal component luminosity in the same passband. This is below observed values from Cen X−4 and Aql X−1(Asai et al. 1996b; Rutledge et al. 2001b; Campana et al. 2000; Rutledge et al. 2001a). The absence of a stronger power-law component is due in part to our spectral selection, requiring R_∞=13 km thermal sources.

2.1. Astrometric Correction

Carson et al. (2000; C00 hereafter) examined three ROSAT/HRI sources (A, B and C) in the GC core, and optically identified CVs spatially coincident with two of them. Their Star A (Table 1 in C00) corresponds to our source #4; their Star B is our source #6. The optical separation of C00's CVs is 38.0±0.2″, compared with the X-ray separation of the *Chandra* sources of 37.99±0.03″. We therefore re-assign astrometry on the basis of C00's positions. This astrometry is reflected in the source positions given in Table 1. Prior to re-assignment, the astrometry of star A and B were offset from the *Chandra* pointing

astrometry by (0.0,0.6″) and (0.0,0.8″) in (R.A., dec.), consistent with the absolute pointing accuracy of *Chandra*. This results in a systematic positional uncertainty of 0.15″ for CXOU 132619.7-472910.8, limited by the astrometric accuracy of C00.

3. Properties of the Source #3

We have found in the previous section that the spectral and intensity properties of source #3 are readily explained if the source is a qNS. We examine the source characteristics in more detail in this section.

Its position at 1.7 core radii is perhaps surprising given the expectation of mass segregation expected in the core of GCs (Verbunt & Meylan 1988). However, timing solutions for 15 millisecond pulsars in 47 Tuc place eight of these beyond 1.7 core radii (r_c=23.1±1.7″; Freire et al. 2001), indicating that such a large radius is not uncommon for neutron stars in GCs, as may be expected from exchange interactions with primordial cluster binaries (Hut et al. 1991).

The X-ray sources in NGC 5139 have been observed with *Einstein*, *ROSAT*/PSPC and *ROSAT*/HRI and examined several times (Hertz & Grindlay 1983; Johnston et al. 1994; Cool et al. 1995; Verbunt & Johnston 2000; Verbunt 2001). In some earlier work our source #3 is their source B (Hertz & Grindlay 1983; Cool et al. 1995). Elsewhere, it is source #7 (Johnston et al. 1994; Verbunt & Johnston 2000; Verbunt 2001). None of these works speculated on the classification of (our) source #3. While an earlier paper found this source to be extended (Cool et al. 1995), later, more sensitive work found the object was a point source (Verbunt & Johnston 2000), as do we.

Verbunt & Johnston (2000), V00 hereafter examined 7 HRI observations, taken at 7 different observational epochs (Aug 1992, Jan 1993, Jul 1994, Jan 1995, Jul 1995, Feb 1996

and Jan 1997), and found no evidence for variability in source #3. Dividing the longest observation (74 ksec) into two parts (separated by 10 days), V00 finds the countrates of (1.7±0.3 and 1.1±0.2 c/ksec), which are different by a factor of 1.5±0.4 (that is, consistent with being the same, within a factor of <2.7, 3σ). In comparison, a factor of $\lesssim$3 variability over timescales of days (Campana et al. 1997) to years (Garcia & Callanan 1999; Rutledge et al. 2000, 2001a, 2001b) in field qNSs has been observed. The absence of variability in CXOU 132619.7-472910.8 on a ∼5 year timescale is consistent with the quiescent luminosity being 100% due to a hot thermal core of a qNS.

Finally, we extracted the X-ray counts of source #3 from the 120 ksec of publicly available HRI data [7]; the majority of the integration was collected from three observations (1995 Jan, 17.7 ksec; 1995 Jul, 75.5 ksec; 1996 Feb, 13.0 ksec), collected ≈5 yrs prior to the *Chandra* observation. A joint spectral fit between the *Chandra* spectrum and the HRI observation, using an absorbed H atmosphere spectrum, finds the average HRI countrate is consistent with that predicted by the *Chandra* spectrum, with a ratio of HRI countrate/ACIS predicted countrate of 1.14±0.12 (1σ; or a limit of <50% variability at 3σ confidence).

The number of counts per bin in all 21448 time bins (duration ≈3.24 sec) is consistent with a Poisson distribution. A power-density spectrum (Lewin et al. 1988) of the joined observations also show no power in excess of the Poisson level, with a 3σ upper limit of <25% rms (0.2-10 keV; 10-10^5 sec). Thus, source #3 exhibits no evidence of intensity variability on timescales between 4 sec and 5 yr.

[7]obtained from http://heasarc.gsfc.nasa.gov

4. Discussion and Conclusions

Source #3 (CXOU 132619.7-472910.8) is spectrally consistent with being a quiescent neutron star, and not with being a CV, RS CVn, or MSP. The resulting normalization in a H atmosphere spectral interpretation gives R_∞=14.3±2.1 (D/ 5 kpc) km as a coincidence. The uncertainty in distance to NGC 5139 is conservatively estimated at 10% (S. G. Djorgovski 2001, priv. comm.), which, when we include this in our quoted uncertainty, gives a NS radius of 14.3±2.5 km. We give its best fit H atmosphere spectral parameters in Table 2, along with those from the field sources from our previous studies. The observed bolometric thermal luminosity is $L_{\rm bol,\infty}$ =(5±2)×10^{32} erg s^{-1}. The low value of $kT_{\rm eff}^{\infty}$ – comparable to that of Cen X−4 – may indicate the two have similar outburst timescales (>30 yr in the case of Cen X−4) assuming similar outburst accretion rates, (cf. Eq 1) which may explain the absence of a recorded outburst from CXOU 132619.7-472910.8.

If source #3 were a NLSy1 source, the X-ray spectrum is unusual, in that it is not consistent with a single power-law slope, and we must additionally accept as a coincidence that the intensity should be the same as from a 10 km neutron star at the distance of NGC 5139. Caution must be taken, however, as the source was selected on the basis of its consistency with this radius; it remains to be unequivocally demonstrated that the object in question is indeed a qNS.

We cannot explicitly exclude that source #3 is an unusual MSP, CV, RS CVn or a NLSy1, particularly given that the number of X-ray sources detected in NGC 5139 are comparable to that expected from background AGN. Nonetheless, we conclude the object is most likely a typical example of a field qNSs, rather than an unusual example of another population.

The classification of source #3 as a qNS can be confirmed with an optical identification of the companion, through ellipsoidal variations associated with the binary orbital period,

and by optical spectroscopy revealing an accretion disk (McClintock & Remillard 2000). Naturally, an X-ray outburst would also confirm this classification. If further observations of CXOU 132619.7-472910.8 support its identification as a qNS, this would then be the first qNS identified in quiescence through its spectral properties, rather than through an X-ray outburst.

The apparent absence of a power-law spectral component which has been observed from field qNSs Cen X−4 and Aql X−1 may indicate that this spectral component is not always present in qNSs. It has been suggested that the observed variability in field qNSs is due exclusively to the power-law spectral component (Rutledge et al. 2001b). If so, then the absence of both the power-law component and intensity variability in source #3 is consistent with its identification as a qNS. Because we do not include a power-law component in our spectral modeling, we may have missed additional qNSs in this GC, which are nonetheless detected with *Chandra*.

The identification of previously unknown qNSs in globular clusters through their quiescent X-ray spectra opens up new observational opportunities for this class of sources. As discussed in Rutledge et al. (2000), the distances to GCs post-*Hipparcos* can be measured to as little as 3% uncertainty (see, for example, Carretta et al. 2000). This is far superior to the sometimes 50-100% uncertainty in the source distances for field qNSs. Combined with an accurate measurement of the qNS angular size obtained with X-ray spectroscopy of the thermal H atmosphere, one then can produce precision measurements of NS radii. The value of such measurements was highlighted recently by Lattimer & Prakash (2001), who showed that one NS radius measurement of ± 1 km accuracy could potentially exclude nearly half of the proposed nuclear equations of state.

The radius measurements of NSs in GCs would be limited in accuracy by the signal-to-noise of the spectrum and the systematic uncertainty in the intrinsic spectrum, rather than

the uncertainty in source distance. The backside-illuminated ACIS-S detector on *Chandra* (which has higher sensitivity at energies below 1 keV) would produce a factor of 2.5 higher countrate than the ACIS-I for the observed spectrum of CXOU 132619.7-472910.8; in 70 ksec, this would measure R_∞/D to 8%(1σ) if $N_{\rm H}$ is assumed *a priori* ($\pm$20-35% if one does not assume the $N_{\rm H}$ value). The *XMM*/pn detector would produce a factor of 5 higher countrate than ACIS-I, over a similar passband, with subsequent improvement on the derived R_∞/D. With *Con-X*, CXOU 132619.7-472910.8 would produce 11000 counts in a 30 ksec observation sufficient to measure R_∞/D to $\pm$7%, including uncertainty in all spectral parameters ($N_{\rm H}$, $kT_{\rm eff}$, R_∞/D, and a power-law α and normalization). Combined, with a 3% uncertainty in distance to the GC, R_∞ would be measured to $\pm$ 8% ($\pm$1 km for R_∞=13 km). Thus, a program measuring the radii of transient neutron stars in quiescence in GCs would usefully constrain the NS equation of state.

The authors continue to be grateful to the *Chandra* Observatory team for producing this exquisite observatory. This research was partially supported by the National Science Foundation under Grant No. PHY99-07949 and by NASA through grant NAG 5-8658 and NAG 5-7017. GGP acknowledges support through NAG5-10865. L. B. is a Cottrell Scholar of the Research Corporation. E. F. B. acknowledges support from an Enrico Fermi Fellowship.

References

Arnaud, K. A., 1996, in G. Jacoby & J. Barnes (eds.), *Astronomical Data Analysis Software and Systems V.*, Vol. 101, p. 17, ASP Conf. Series

Asai, K., Dotani, T., Hoshi, R., Tanaka, Y., Robinson, C. R., & Terada, K., 1998, PASJ 50, 611

Asai, K., Dotani, T., Mitsuda, K., Hoshi, R., Vaughan, B., Tanaka, Y., & Inoue, H., 1996b, PASJ 48, 257

Bailyn, C. D., Grindlay, J. E., & Garcia, M. R., 1990, ApJ 357, L35

Bildsten, L. & Rutledge, R. E., 2000, *The Neutron Star – Black Hole Connection*, Kouveliotou et al (eds.) (NATO ASI Elounda 1999); astro-ph/0005364

Boller, T., Brandt, W. N., & Fink, H., 1996, A&A 305, 53

Brown, E. F., Bildsten, L., & Rutledge, R. E., 1998, ApJ 504, L95, [BBR98]

Campana, S., Colpi, M., Mereghetti, S., Stella, L., & Tavani, M., 1998a, A&A Rev. 8, 279

Campana, S., Mereghetti, S., Stella, L., & Colpi, M., 1997, A&A 324, 941

Campana, S., Stella, L., Mereghetti, S., Colpi, M., Tavani, M., Ricci, D., Fiume, D. D., & Belloni, T., 1998b, ApJ 499, L65

Campana, S., Stella, L., Mereghetti, S., & Cremonesi, D., 2000, A&A 358, 583

Carretta, E., Gratton, R. G., Clementini, G., & Fusi Pecci, F., 2000, ApJ 533, 215

Carson, J. E., Cool, A. M., & Grindlay, J. E., 2000, ApJ 532, 461

Chen, W., Shrader, C. R., & Livio, M., 1997, ApJ 491, 312

Colpi, M., Geppert, U., & Page, D., 2000, ApJ 529, L29

Cool, A. M., Grindlay, J. E., Bailyn, C. D., Callanan, P. J., & Hertz, P., 1995, ApJ 438, 719

Dempsey, R. C., Linsky, J. L., Schmitt, J. H. M. M., & Fleming, T. A., 1993, ApJ 413, 333

Dickey, J. M. & Lockman, F. J., 1990, ARA&A 28, 215

Djorgovski, S. G. & Meylan, G., 1993, ASP Conf. Ser. 50: Structure and Dynamics of Globular Clusters

Eracleous, M., Halpern, J., & Patterson, J., 1991, ApJ 382, 290

Forman, W., Jones, C., & Tananbaum, H., 1976, ApJ 207, L25

Freire, P. C., Camilo, F., Lorimer, D. R., Lyne, A. G., Manchester, R. N., & D'Amico, N., 2001, MNRAS, submitted, astro-ph/0103372

Garcia, M. R. & Callanan, P. J., 1999, AJ 118, 1390

Giacconi, R., Rosati, P., Tozzi, P., Nonino, M., Hasinger, G., Norman, C., Bergeron, J., Borgani, S., Gilli, R., Gilmozzi, R., & Zheng, W., 2001, ApJ 551, 624

Grindlay, J., Edmonds, P., Heinke, C., & Murray, S., 2001, *Science*, in press

Haensel, P. & Zdunik, J. L., 1990, A&A 227, 431

Harris, W. E., 1996, AJ 112, 1487

Hasinger, G., Burg, R., Giacconi, R., Schmidt, M., Truemper, J., & Zamorani, G., 1998, A&A 329, 482

Hasinger, G., Lehmann, I., Schmidt, M., Gunn, J. E., Schneider, D. P., Giacconi, R., Trümper, J., & Zamorani, G., 2000, *New Astronomy Review* 44, 497

Hertz, P. & Grindlay, J. E., 1983, ApJ 267, L83

Hut, P., Murphy, B. W., & Verbunt, F., 1991, A&A 241, 137

in 't Zand, J. J. M., Verbunt, F., Strohmayer, T. E., Bazzano, A., Cocchi, M., Heise, J., van Kerkwijk, M. H., Muller, J. M., Natalucci, L., Smith, M. J. S., & Ubertini, P., 1999, A&A 345, 100

Johnston, H. M., Verbunt, F., & Hasinger, G., 1994, A&A 289, 763

Lattimer, J. M. & Prakash, M., 2001, ApJ 550, 426

Lee, Y. ., Joo, J. ., Sohn, Y. ., Rey, S. ., Lee, H. ., & Walker, A. R., 1999, Nature 402, 55

Lemen, J. R., Mewe, R., Schrijver, C. J., & Fludra, A., 1989, ApJ 341, 474

Lewin, W. H. G., Doty, J., Clark, G. W., Rappaport, S. A., Bradt, H. V. D., Doxsey, R., Hearn, D. R., Hoffman, J. A., Jernigan, J. G., Li, F. K., Mayer, W., McClintock, J., Primini, F., & Richardson, J., 1976, ApJ 207, L95

Lewin, W. H. G., Van Paradijs, J., & Van der Klis, M., 1988, *Space Science Reviews* 46, 273

Majewski, S. R. & et. al., 1999, Proceedings of the 35th Liege International Astrophysics Colloquium: The Galactic Halo: From Globular Clusters to Field Stars, July 5-8, 1999; astro-ph/9910278

McClintock, J. E. & Remillard, R. A., 2000, ApJ 531, 956

Mineo, T., Cusumano, G., Kuiper, L., Hermsen, W., Massaro, E., Becker, W., Nicastro, L., Sacco, B., Verbunt, F., Lyne, A. G., Stairs, I. H., & Shibata, S., 2000, A&A 355, 1053

Pooley, D., Lewin, W. H. G., Verbunt, F., Fox, D. W., Margon, B., Kaspi, V. M., van der Klis, M., & Miller, J., 2000, *AAS/High Energy Astrophysics Division* 32, 2901

Press, W., Flannery, B., Teukolsky, S., & Vetterling, W., 1995, *Numerical Recipies in C*, Cambridge University Press

Rajagopal, M. & Romani, R. W., 1996, ApJ 461, 327

Rots, A. H., Jahoda, K., Macomb, D. J., Kawai, N., Saito, Y., Kaspi, V. M., Lyne, A. G., Manchester, R. N., Backer, D. C., Somer, A. L., Marsden, D., & Rothschild, R. E., 1998, ApJ 501, 749

Rutledge, R. E., Bildsten, L., Brown, E. F., Pavlov, G. G., & Zavlin, V. E., 1999, ApJ 514, 945

Rutledge, R. E., Bildsten, L., Brown, E. F., Pavlov, G. G., & Zavlin, V. E., 2000, ApJ 529, 985

Rutledge, R. E., Bildsten, L., Brown, E. F., Pavlov, G. G., & Zavlin, V. E., 2001a, ApJ, accepted

Rutledge, R. E., Bildsten, L., Brown, E. F., Pavlov, G. G., & Zavlin, V. E., 2001b, ApJ

551, 921

Saito, Y., Kawai, N., Kamae, T., Shibata, S., Dotani, T., & Kulkarni, S. R., 1997, ApJ 477, L37

Swank, J. H., Holt, S. S., White, N. E., & Becker, R. H., 1981, ApJ 246, 208

Takahashi, M., Shibata, S., Torii, K., Saito, Y., & Kawai, N., 1998, IAU Circ. 7030, 3

Verbunt, F., 2001, A&A 368, 137

Verbunt, F., Elson, R., & Van Paradijs, J., 1984, MNRAS 210, 899

Verbunt, F. & Johnston, H. M., 2000, A&A 358, 910

Verbunt, F. & Meylan, G., 1988, A&A 203, 297

Verbunt, F., van Kerkwijk, M. H., in't Zand, J. J. M., & Heise, J., 2000, A&A 359, 960

Zavlin, V. E. & Pavlov, G. G., 1998, A&A 329, 583

Zavlin, V. E., Pavlov, G. G., & Shibanov, Y. A., 1996, A&A 315, 141

Fig. 1.— The νF_ν model spectrum of CXOU 132619.7-472910.8 (Source #3), observed with the ACIS-I. The solid line is the best-fit unabsorbed H atmosphere model spectrum, with $N_{\rm H,22}$=0.09 held fixed (that is, the intrinsic X-ray spectrum, prior to absorption by the interstellar medium; see Table 2). The cross points are the background subtracted observational PHA spectrum, covering the energy ranges, with the error bars taken from count rates.

Fig. 2.— Best-fit H atmosphere spectral parameters for spectroscopy sources, compared with the field qNSs. Points are marked with source number, and 1σ error bars (field sources have 90% confidence error bars) are the best-fit $kT_{\rm eff}^{\infty}$ and R_∞, with $kT_{\rm eff}^{\infty}$ limited for this fit at 410 eV. The broken line marks the approximate flux limit for a H atmosphere source ($\propto {R_\infty}^2 {kT_{\rm eff}^{\infty}}^4$). Source #3 overlaps in R_∞ with field qNSs Aql X−1, Cen X−4, 2129+47 and 1608-522. Source numbers in the upper-right box did not produce statistically acceptable fits. The connected points for 2129+47 and 1608-522 are for two different assumptions of distance and $N_{\rm H}$ (see Rutledge et al. 1999, 2000).

Fig. 3.— Comparison between the EM (in arbitrary units) vs. $kT_{\rm Bremss.}$ of field CVs from E91 (solid squares), and source #3 and #31 (as marked). Source #3 is spectrally softer than all other CVs observed by E91, and has the highest EM.

Fig. 4.— Comparison of EM_1 vs. EM_2/EM_1 between RS CVns (D93) and sources #3 and #31. The RS CVn EM_2/EM_1 values are the best-fit values (D93), while the qNSs' EM_2/EM_1 values are 90% confidence upper-limits. The implied values of EM_1 for all but #36 are significantly higher than observed from field RS CVns. The upper-limits EM_2/EM_1 are below the values measured from field RS CVns in source #3, but not source #31.

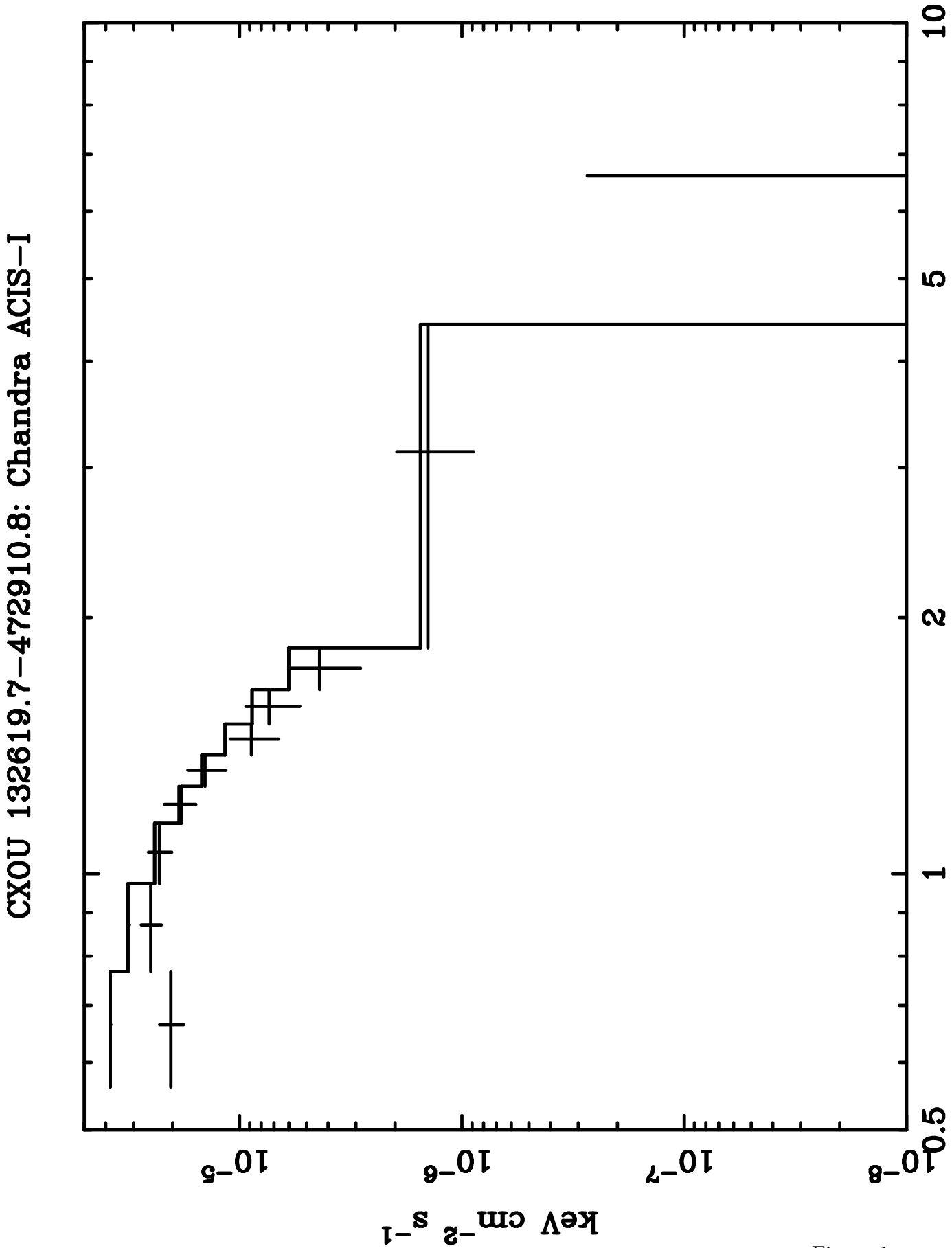
CXOU 132619.7−472910.8: Chandra ACIS−I
keV cm^{-2} s^{-1}
10^{-5}
10^{-6}
10^{-7}
10^{-8}
0.5
1
2
5
10
Energy (keV)

Figure 1

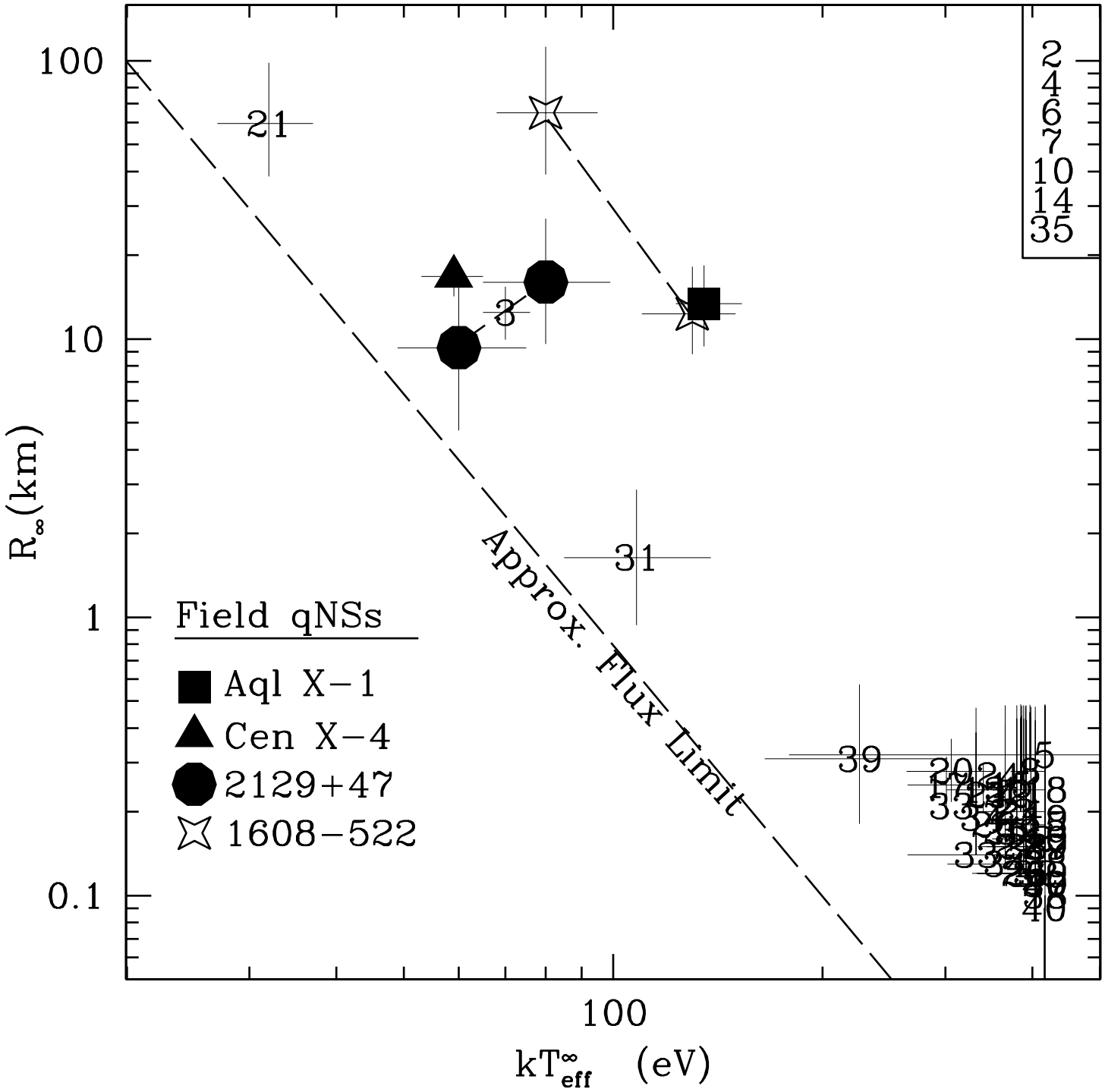
100
10
1
0.1
R_∞ (km)
100
kT^∞_{eff} (eV)
Field qNSs
Aql X−1
Cen X−4
2129+47
1608−522
Approx. Flux Limit
21
3
31
39
2
4
6
7
10
14
35

Figure 2

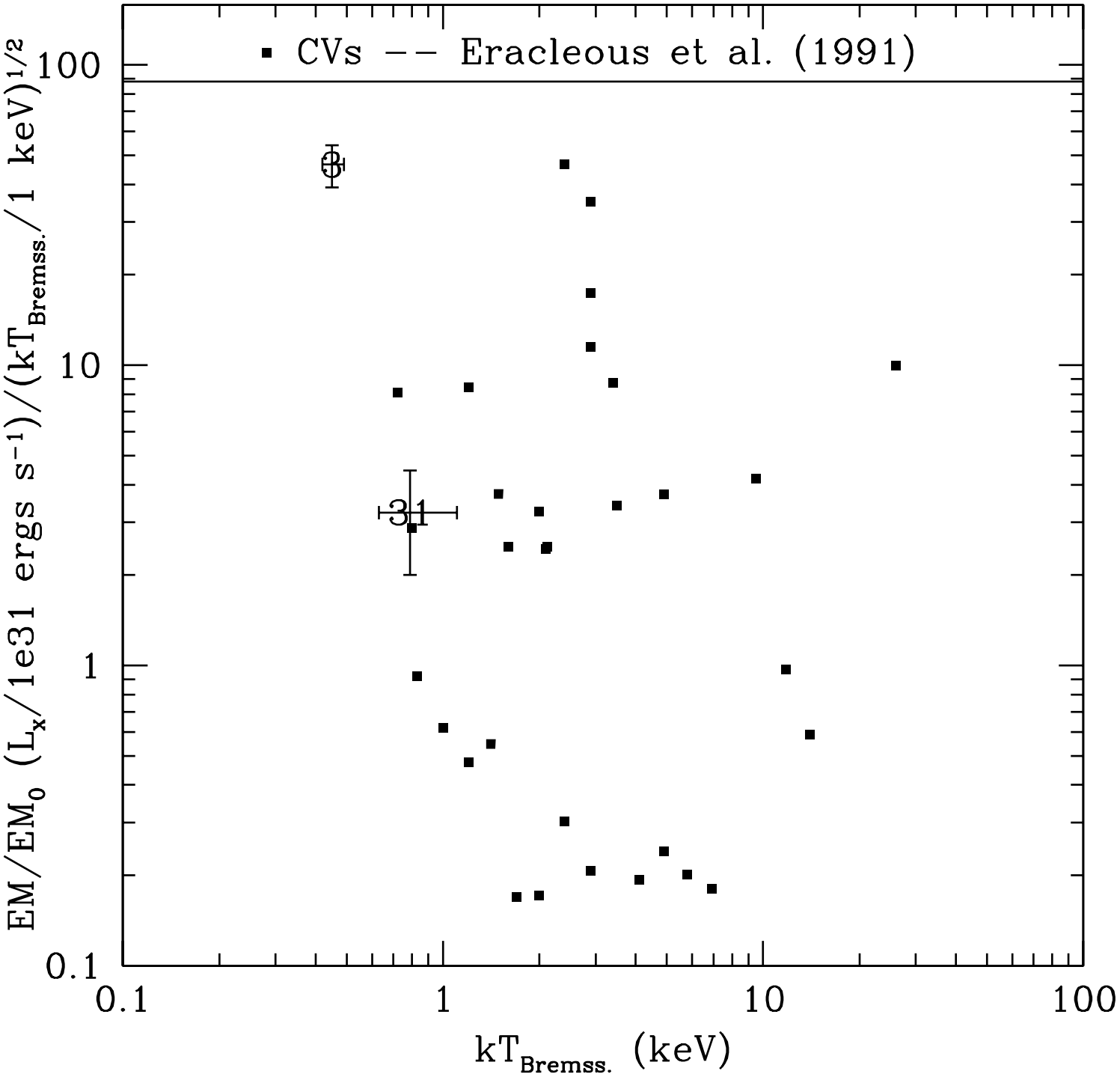
CVs -- Eracleous et al. (1991)
EM/EM$_0$ (L$_x$/1e31 ergs s^{-1})/(kT$_{Bremss.}$/1 keV)$^{1/2}$
kT$_{Bremss.}$ (keV)
0.1
1
10
100
Θ
31

Figure 3

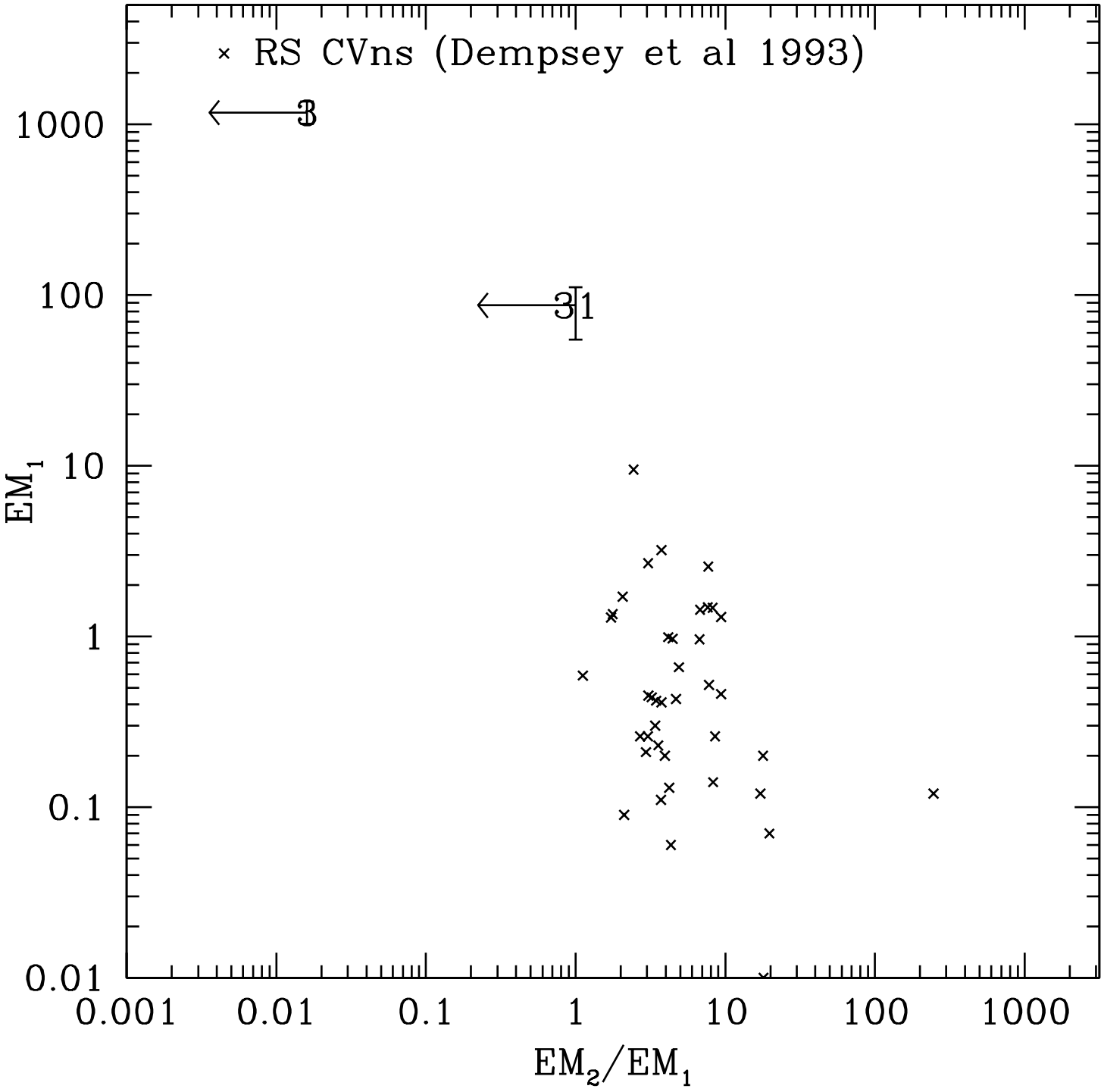
× RS CVns (Dempsey et al 1993)
1000
100
10
1
0.1
0.01
EM1
0.001
0.01
0.1
1
10
100
1000
EM2/EM1

Figure 4

Table 1. *Chandra* X-ray Sources in the Field of NGC 5139

ID	SNR	R.A. (J2000)	Dec. (J2000)	Stat. δ^a ($''$)	Δ/r_c [e]	χ^2_ν/dof (prob)	$kT^{\infty}_{\rm eff}$ (eV)	I c/ksec (±)	Type[b]	ref.
1	53.3	13 25 52.211	-47 19 8.05	±0.17	5.04	... [d]	–	50.7 (1.6)	dMe	1
2	21.6	13 26 1.531	-47 33 6.67	±0.14/±0.18	3.35	226/3 (n/a)	–	13.4 (0.5)	–	
3	20.1	13 26 19.757	-47 29 11.51	±0.03/±0.05	1.71	2.61/3 (0.050)	72±1	6.9 (0.4)	qNS	3
4	19.8	13 26 52.134	-47 29 36.29	±0.02	0.56	105/3 (n/a)	–	9.9 (0.4)	CV	2
5	18.4	13 26 54.496	-47 22 5.34	±0.10/±0.08	2.57	78/3 (n/a)	–	7.9 (0.4)	–	
6	17.5	13 26 53.503	-47 29 0.92	±0.02	0.52	117/3 (n/a)	–	10.2 (0.4)	CV	2
7	16.2	13 27 29.326	-47 25 54.92	±0.16/±0.12	3.00	44/3 (9×10^{-29})	–	6.0 (0.3)	–	
8	15.0	13 27 12.887	-47 34 57.79	±0.17	3.00	51/3 (10^{-33})	–	5.3 (0.3)	–	
[c] 9	14.5	13 25 30	-47 15 24	···	7.05	... [d]	–	7.3 (0.7)	–	
10	13.3	13 26 20.336	-47 30 3.92	±0.06/±0.08	1.75	76/3 (n/a)	–	4.5 (0.3)	–	
11	12.8	13 27 11.785	-47 32 41.43	±0.12/±0.10	2.30	41/3 (10^{-26})	–	3.8 (0.3)	–	
12	11.7	13 26 11.503	-47 34 4.81	±0.28	3.06	... [d]	–	2.9 (0.2)	–	
13	10.3	13 26 44.106	-47 32 32.31	±0.07	1.51	24/3 (10^{-15})	–	2.5 (0.2)	–	
14	10.1	13 27 27.495	-47 31 33.41	±0.21	2.92	8.57/3 (10^{-05})	–	2.7 (0.2)	–	
15	9.6	13 26 25.089	-47 32 28.51	±0.09/±0.12	2.00	24/3 (4×10^{-16})	–	2.5 (0.2)	–	
[c] 16	9.3	13 25 38.4	-47 17 51	···	6.03	... [d]	–	4.3 (0.5)	–	
17	9.0	13 26 37.412	-47 30 53.95	±0.05	1.04	20/3 (4×10^{-13})	–	1.7 (0.2)	–	
18	8.7	13 26 48.640	-47 27 45.75	±0.03	0.37	... [d]	–	2.9 (0.2)	–	
19	8.5	13 26 41.448	-47 22 16.79	±0.18	2.45	33/3 (2×10^{-21})	–	2.0 (0.2)	–	
20	8.4	13 25 57.393	-47 32 51.72	±0.47	3.54	14.78/3 (10^{-09})	–	2.0 (0.2)	–	
21	8.1	13 26 46.014	-47 19 45.40	±0.52/±0.40	3.40	7.57/3 (5×10^{-05})	–	1.8 (0.2)	–	
22	7.8	13 26 27.510	-47 34 57.66	±0.29	2.71	22/3 (8×10^{-15})	–	1.9 (0.2)	–	
23	7.6	13 26 48.717	-47 31 26.09	±0.07	1.10	18/3 (3×10^{-12})	–	1.6 (0.2)	–	
24	7.4	13 26 23.500	-47 19 22.09	±0.48/±0.66	3.84	18/3 (5×10^{-12})	–	2.3 (0.2)	–	
25	6.2	13 26 34.310	-47 30 34.50	±0.08	1.06	11.76/3 (10^{-07})	–	1.0 (0.1)	–	
26	6.2	13 26 55.078	-47 31 14.49	±0.09	1.17	14.89/3 (10^{-09})	–	1.0 (0.1)	–	
27	6.2	13 27 21.200	-47 23 23.73	±0.38	3.05	18/3 (6×10^{-12})	–	1.2 (0.2)	–	
28	6.1	13 26 13.561	-47 34 40.63	±0.45	3.13	... [d]	–	1.2 (0.2)	–	
29	6.1	13 26 51.057	-47 31 45.64	±0.08	1.25	16/3 (5×10^{-11})	–	1.1 (0.1)	–	
30	6.0	13 26 39.240	-47 36 30.25	±0.65	3.06	... [d]	–	1.6 (0.2)	–	
31	6.0	13 26 38.258	-47 19 57.00	±0.65	3.36	1.70/3 (0.165)	50±1	1.0 (0.2)	–	
32	5.8	13 27 28.290	-47 24 24.86	±0.55/±0.44	3.19	11.78/3 (10^{-07})	–	1.0 (0.1)	–	
33	5.5	13 26 49.559	-47 32 13.62	±0.12	1.41	8.65/3 (10^{-05})	–	0.7 (0.1)	–	
34	5.5	13 27 7.998	-47 23 34.23	±0.22	2.41	11.77/3 (10^{-07})	–	0.8 (0.1)	–	
35	5.5	13 27 10.001	-47 33 21.99	±0.26/±0.36	2.40	23/3 (3×10^{-15})	–	1.4 (0.2)	–	
[c] 36	5.5	13 25 42.7	-47 19 16	···	5.45	... [d]	–	1.3 (0.3)	–	
37	5.4	13 26 26.964	-47 34 10.57	±0.24/±0.33	2.46	17/3 (4×10^{-11})	–	1.1 (0.1)	–	
38	5.1	13 26 59.191	-47 34 59.26	±0.36	2.60	9.04/3 (6×10^{-06})	–	1.0 (0.1)	–	
39	5.1	13 26 12.686	-47 24 13.71	±0.31/±0.41	2.74	6.00/3 (4×10^{-04})	–	0.9 (0.1)	–	
40	5.1	13 27 6.416	-47 25 38.76	±0.22/±0.18	1.75	9.00/3 (6×10^{-06})	–	0.7 (0.1)	–	

Note. — [a] Statistical uncertainty in R.A./Dec. (or, both), in arcsec. Systematic positional uncertainty is $\pm0.15''$ (see text). [b] Type: qNS= quiescent transient neutron star; CV= cataclysmic variable; [c] X-ray *celldetect* positional uncertainty possibly incorrect by up to $10''$due to large off-axis angle and low S/N; [d] Object not spectrally analysed (see text); [e] r_c=$156''$(Djorgovski & Meylan 1993); 1, Cool et al. (1995); 2, Carson et al. (2000); 3, present work;

Table 2. H Atm. Spectral Parameters for CXOU 132619.7-472910.8 and Field qNSs

Object	R_∞ (km)		$kT_{\rm eff}^\infty$ (eV)	$N_{\rm H}$ (10^{22} cm^{-2})	Ref.
CXOU 132619.7-472910.8	14.3±2.1	(D/5 kpc)	66^{+4}_{-5}	(0.09)	0
Aql X−1	13.4^{+5}_{-4}	(D/5 kpc)	135^{+18}_{-12}	$0.35^{+0.08}_{-0.07}$	1
Cen X−4	16.8±2.6	(D/1.2 kpc)	59±6	(0.055)	2
[a] 4U 2129+47	$9.3^{+7.8}_{-4.6}$	(D/1.5 kpc)	60^{+15}_{-11}	(0.28)	3
[a] 4U 2129+47	$16^{+11}_{-6.4}$	(D/6.0 kpc)	80^{+19}_{-15}	(0.17)	3
[a] 4U 1608-522	$12.3^{+5.9}_{-3.5}$	(D/3.6 kpc)	130±20	(0.8)	4
[a] 4U 1608-522	65^{+47}_{-26}	(D/3.6 kpc)	80^{+15}_{-12}	(1.5)	4

Note. — Error bars are 90% confidence. Values in parenthesis are assumed. Previously measured values have been converted from R and $kT_{\rm eff}$ to R_∞ and $kT_{\rm eff}^\infty$ (values as appear at infinity); 0, present work; 1, Rutledge et al. (2001a); 2, Rutledge et al. (2001b); 3, Rutledge et al. (2000); 4, Rutledge et al. (1999); [a] Different assumed values of D and/or $N_{\rm H}$.